Surgical Endoscopy (2021) 35:1844–1850
https://doi.org/10.1007/s00464-020-07586-5

Hyperspectral enhanced reality (HYPER) for anatomical liver resection

Takeshi Urade[1] · Eric Felli[1,2] · Manuel Barberio[1,2] · Mahdi Al-Taher[1] · Emanuele Felli[3] · Laurent Goffin[4] · Vincent Agnus[1] · Giuseppe Maria Ettorre[5] · Jacques Marescaux[1,6] · Didier Mutter[1,3,6] · Michele Diana[1,2,3,4,6]

Received: 23 February 2020 / Accepted: 22 April 2020 / Published online: 27 April 2020

Abstract

Background Clinical evaluation of the demarcation line separating ischemic from non-ischemic liver parenchyma may be challenging. Hyperspectral imaging (HSI) is a noninvasive imaging modality, which combines a camera with a spectroscope and allows quantitative imaging of tissue oxygenation. Our group developed a software to overlay HSI images onto the operative field, obtaining HSI-based enhanced reality (HYPER). The aim of the present study was to evaluate the accuracy of HYPER to identify the demarcation line after a left vascular inflow occlusion during an anatomical left hepatectomy.

Materials and methods In the porcine model ($n=3$), the left branches of the hepatic pedicle were ligated. Before and after vascular occlusion, HSI images based on tissue oxygenation (StO_2), obtained through the Near-Infrared index (NIR index), were regularly acquired and superimposed onto RGB video. The demarcation line was marked on the liver surface with electrocautery according to HYPER. Local lactates were measured on blood samples from the liver surface in both ischemic and perfused segments using a strip-based device. At the same areas, confocal endomicroscopy was performed.

Results After ligation, HSI demonstrated a significantly lower oxygenation (NIR index) in the left medial lobe (LML) ($0.27\% \pm 0.21$) when compared to the right medial lobe (RML) ($58.60\% \pm 12.08$; $p=0.0015$). Capillary lactates were significantly higher (3.07 mmol/L ± 0.84 vs. 1.33 ± 0.71 mmol/L; $p=0.0356$) in the LML versus RML, respectively. Concordantly, confocal videos demonstrated the absence of blood flow in the LML and normal perfusion in the RML.

Conclusions HYPER has made it possible to correctly identify the demarcation line and quantify surface liver oxygenation. HYPER could be an intraoperative tool to guide perfusion-based demarcation line assessment and segmentation.

Keywords Enhanced reality · Hepatectomy · Hyperspectral imaging · Image-guided surgery

Takeshi Urade and Eric Felli equally contributed to this work.

Electronic supplementary material The online version of this article (https://doi.org/10.1007/s00464-020-07586-5) contains supplementary material, which is available to authorized users.

✉ Michele Diana
michele.diana@ircad.fr; michele.diana@ihu-strasbourg.eu

1 Institute of Image-Guided Surgery, IHU-Strasbourg, Strasbourg, France

2 Institute of Physiology, EA3072 Mitochondria Respiration and Oxidative Stress, University of Strasbourg, Strasbourg, France

3 Department of General, Digestive, and Endocrine Surgery, University Hospital of Strasbourg, Strasbourg, France

4 ICube/CNRS, University of Strasbourg, Strasbourg, France

5 Department of Transplantation and General Surgery, San Camillo Hospital, Rome, Italy

6 Research Institute against Digestive Cancer, IRCAD, 1, place de l'Hôpital, 67091 Strasbourg, France

Anatomical liver resections (ALRs) are performed by removing a section of the liver visually identified via surface color changes due to selective blood inflow occlusion or staining of the portal tract [1–3]. The resulting demarcation line discriminates the boundaries between ischemic and non-ischemic tissue.

This eye-based evaluation suffers from being operator-dependent and from the inability to quantify local oxygenation, particularly beneath the liver surface. Moreover, the inhomogeneity in surface perfusion appreciation in pathologic conditions, including cirrhosis, steatosis, fibrosis, has been the driver for the development of intraoperative imaging methods such as fluorescence-based segmentation, by means of administration of a fluorophore, mostly Indocyanine Green (ICG) [4].

There are two staining methods to identify anatomical hepatic regions with ICG. Positive staining method is performed to detect anatomical hepatic regions by injection of

ICG into the portal branches under IOUS guidance [4–6], and negative staining method is performed to detect anatomical hepatic regions, as the non-fluorescing ones, by the intravenous injection of ICG after clamping the portal branches [5, 7–10]. However, those methods are limited by the need of injecting an exogenous fluorescent molecule to the patient.

Hyperspectral imaging (HSI) is a contrast-free optical imaging modality which combines a photo camera and a spectroscope [11]. HSI performs spectral analysis of tissues and allows tumor identification [12, 13], organ perfusion assessment [14, 15], and identification of key anatomical structures intraoperatively [16]. HSI systems build images based on the computation of light-tissue interactions phenomena, which depend on the tissue concentration of various compounds, up to a certain depth. In the present experiment, we have used a CMOS push-broom scanning hyperspectral camera (TIVITA®, Diaspective Vision GmbH, Germany). The TIVITA® has preset algorithms, which allow to quantify the relative oxygen saturation (StO_2%) of the superficial microcirculation at a depth up to ~ 1 mm, whereas it is possible to quantify the relative oxygen saturation in deeper layers, within the near-infrared (NIR) spectrum, with a penetration depth up to 4-6 mm. The tissue water index (TWI) can be used to quantify and image the distribution of water in the observed region of interest (ROI) [17].

The majority of the commercially available HSI systems do not provide an effective video rate and the HSI information is provided as a static side-by-side image. In an attempt to overcome this limitation and improve the use of HSI as a surgical navigation tool, our group has introduced the concept of HYPerspectral Enhanced Reality (HYPER) [18]. HYPER is based on the superimposing of static HSI images onto an intraoperative video, using augmented reality technologies. Through the mixed reality, information-rich images are overlaid directly on the screen, providing an effective surgical navigation tool. In analogy to our previous experience in bowel ischemia detection and quantification, we hypothesized that HYPER could precisely identify the future liver demarcation line. The aim of this experimental study was to evaluate the feasibility of HYPER-guided ALR and to assess the accuracy in discriminating ischemic from non-ischemic liver tissue.

Materials and methods

Animals

The present study, which is part of the ELIOS project (Endoscopic Luminescent Imaging for Oncology Surgery), was approved by the local Ethical Committee on Animal Experimentation (ICOMETH No. 38.2016.01.085), and by the French Ministry of Superior Education and Research (MESR) (APAFIS#8721-2017013010316298-v2). All animals used in the experimental laboratory were managed according to French laws for animal use and care, and according to the directives of the European Community Council (2010/63/EU) and ARRIVE guidelines [19]. Three adult male swine (*Sus scrofa* ssp. *domesticus*, mean weight: 24.7 ± 0.5 kg) were housed and acclimatized for 48 h in an enriched environment, respecting circadian cycles of light-darkness, and with constant humidity and temperature conditions. They were fasted 24 h before surgery, with ad libitum access to water, and finally sedated (zolazepam + tiletamine 10 mg/kg IM) 30 min before the procedure to decrease stress. Anesthesia induction was achieved by means of intravenous (18 G IV catheter in ear vein) propofol 3 mg/kg and maintained with rocuronium 0.8 mg/kg along with inhaled isoflurane 2%. At the end of the protocol, animals were euthanized with a lethal dose of pentobarbital (40 mg/kg).

Surgical procedure

The abdominal cavity was accessed via a midline laparotomy. The round ligament, the thin transparent membranes around the liver, and the hepato-gastric ligament were cut to prevent any unexpected traction injuries. During hepatic pedicle dissection, the left hepatic artery and the left portal vein were ligated with 3/0 and 2/0 braided threads, respectively. The demarcation line produced between the right medial (RML) and left medial lobe (LML) was marked on the liver surface with electrocautery following our proprietary software HSI-based enhanced reality (HYPER). The schematic of the set-up in Fig. 1 shows the position of the screen, which allowed the surgeon to follow HYPER and to guide the demarcation line incision. Parenchymal transection was performed to verify if the intraparenchymal perfusion boundaries were matching with the demarcation line suggested by HSI. A clamp crushing method was applied with a special clamp for liver parenchymal transection (Takayama's forceps for liver transection, Yufu Itonaga Co., Ltd., Tokyo, Japan) and a bipolar vessel-sealing device (LigaSure™ Maryland, Covidien, Mansfield, MA, USA). During transection, an intermittent Pringle's maneuver was also performed with a cycle of 15-min clamping with 5 min of perfusion. Finally, hepatic veins were divided with staplers (Endo GIA™, Covidien, Mansfield, MA, USA) and the left median and left lateral lobes were removed.

HSI and HYPER

A commercially available hyperspectral camera (TIVITA®, Diaspective Vision GmbH, Germany) was used to provide intraoperative imaging and quantification of StO_2, NIR perfusion index, and TWI. The TIVITA® was customized

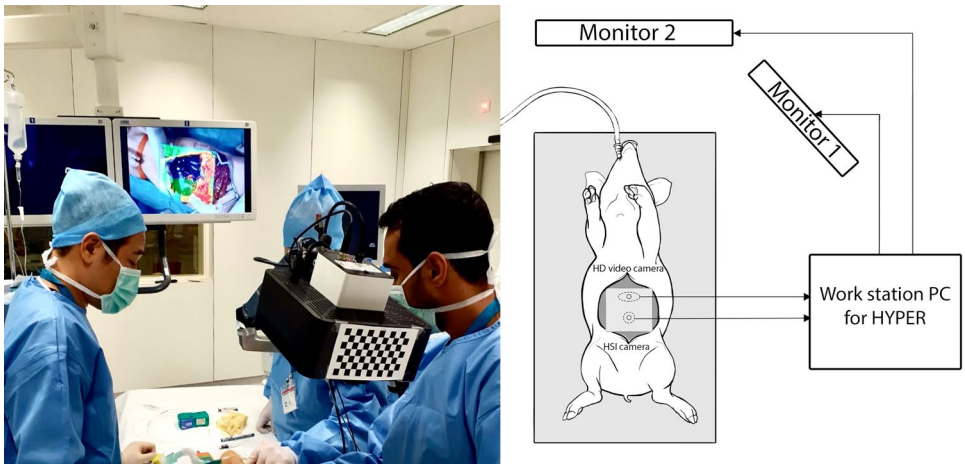

Fig. 1 Schematic of the hyperspectral imaging (HSI)-based enhanced reality (HYPER) system set-up. The workstation PC for HYPER is equipped with TIVITA® software and original software for enhanced reality. The static HSI image is displayed on monitor 1, and the superimposed HSI image on the running video is displayed on monitor 2

integrating an HD video camera (C920 1080p HD Pro Webcam, Logitech, Switzerland). Intrinsic parameters of the hyperspectral camera and of the additional webcam were computed independently, before the procedure. To compute the registration transformation (extrinsic calibration), several poses of a checkerboard are detected simultaneously in both cameras. Checkerboard corners are used to estimate the transformation and to estimate the error. The HSI system requires 6 s to acquire the tissue spectrum analysis and convert into images depending on the preset algorithms (StO_2%, TWI, NIR). Those images are simultaneously displayed side-by-side. For surgical guidance, the HSI-NIR perfusion index was selected to highlight the resulting demarcation line, following vascular ligature, because of the deeper tissue penetration, when compared to the StO_2 index. The accuracy of perfusion evaluation between NIR% and StO_2 was compared post hoc. A NIR perfusion map (low perfusion (blue)/high perfusion (red) colormap) was superimposed on each live video and was displayed on the screen to guide the resection line in enhanced reality. Four electro-cauterized dots on the liver surface, visible in the RGB and NIR images, were used as landmarks to test the accuracy of the registration and to enable an updated registration in case of a novel HSI image acquisition. Ventilation was stopped during HSI images acquisition. The mean value of the HSI parameters (StO_2%, NIR and TWI) was computed on the whole surface of the liver, for each region of interest, before and after ligation.

Probe-based confocal laser endomicroscopy (pCLE)

A Cellvizio® pCLE system (Mauna Kea Technologies, France) was used for endomicroscopic analysis to assess microcirculation, at the same time points of lactate sampling and HSI imaging. Endomicroscopy was performed by applying the tip of the CLE probe directly on the liver surface before vascular ligation (T0), randomly on Glisson's capsule. After vascular ligation, pCLE was repeated during resection on both sides (ischemic and perfused) of the demarcation line (T1). To obtain confocal images, 2 mL of sodium fluorescein (Fluocyne®, Serb, Paris, France) was injected intravenously. The probe was hold manually and the videos were recorded for 1 min.

Local liver lactates

At the same time points, lactates were measured on blood samples obtained by puncturing the liver surface, using a strip-based portable lactate analyzer (EDGE®, ApexBio, Taipei, Taiwan) on the two sides of the demarcation line (which margin error is ~ 0.35 mmol/L [20]). The correlation between HSI parameters and the local capillary lactates was used as primary outcome to establish the sample size. The calculation was based on our previous experiences with bowel ischemia [18, 21], in which the rho correlation coefficient between HSI-StO_2 and lactates was − 0.7. Applying an alpha at 0.05 with a power of 0.9, the required sample size in terms of paired values is 4. In the present study, 12 paired values StO_2 lactates were obtained in total in three pigs.

Statistical analysis

Statistics were performed using GraphPad 8.3 (GraphPad Software®, San Diego, CA, USA). A Pearson's rho was calculated to correlate local lactates with HSI parameters. Student's *t* test, one-way and two-way ANOVA with Dunnett's multiple comparisons were performed to calculate differences in continuous variables. A p value < 0.05 was considered statistically significant.

Results

The extra time required to register the NIR-derived images was only few seconds. The accuracy of the HYPER registration was subpixel and was around 0.35 pixels. The demarcation line was marked under HYPER guidance during the procedure (Videoclip). The software elaboration of the HSI hypercube is displayed in Fig. 2A. Under white light observation, the demarcation line was not always sharp, especially in one of the three animals. The HSI-NIR picture provided a sharper limit of the ischemic area when compared to StO_2% and TWI% parameters. In the first animal, the demarcation line based on clinical evaluation underestimated the ischemic area, when compared to the HYPER-based one (Fig. 2B). Table 1, the intraoperative data is reported. Briefly, the StO_2% index measured at RML and at the control area of the liver were statistically significantly higher when compared to the LML ($p = 0.0117$ and $p = 0.0130$, respectively). No difference was detected between the control and the RML confirming that the ligation was correctly performed. The NIR% and the TWI index of the LML were both significantly lower when compared to the ones measured at the RML and at the control area. There was no difference between the RML and the control for both indexes. Local lactate was coherently higher in the LML; the difference between the RML and the control when compared to the LML was statistically significant ($p = 0.0356$ and $p = 0.0091$, respectively), where the difference between the RML and the control was not significant. StO_2% and NIR% were statistically significantly different in the control and in the RML. The superficial analysis given by StO_2% was less accurate than the NIR% as shown by the difference

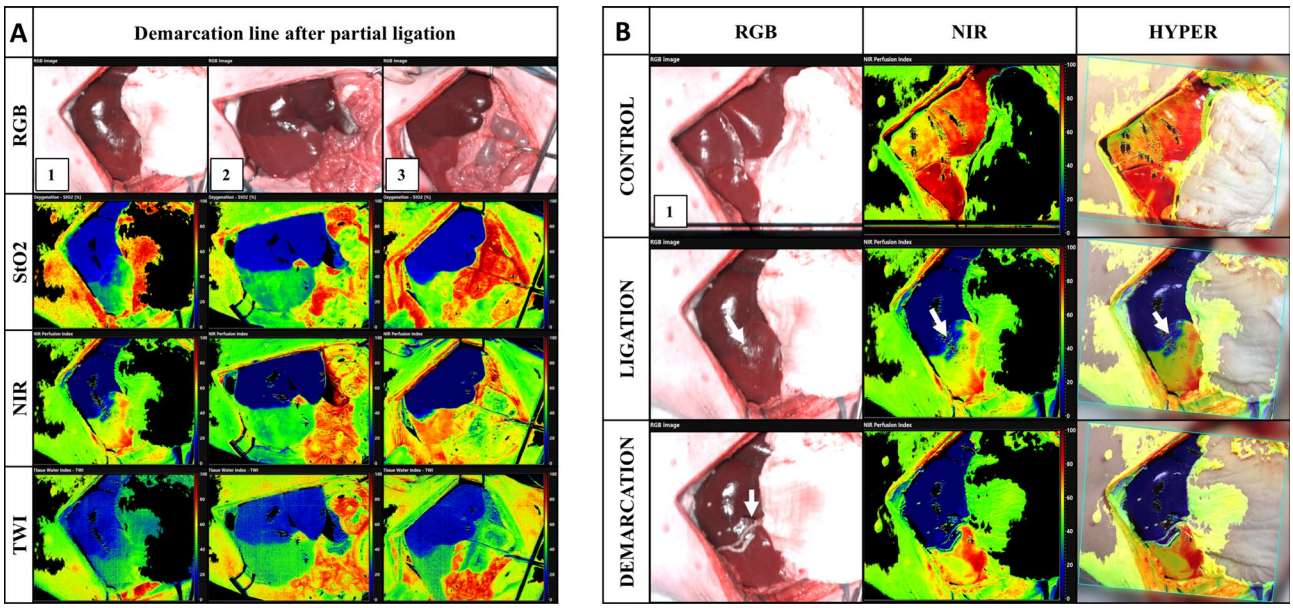

Fig. 2 **A** Hyperspectral liver pictures of the three pig models after the ligation of the left hepatic pedicle branch. **B** Enhanced reality (HYPER) provided by the superimposition of the RGB camera with the Hyperspectral Near-Infrared index obtaining HYPER of pig 1. Unclear demarcation line solved by HSI is highlighted by the white arrows

Table 1 Intraoperative data

Parameter	Control	RML	LML	Control versus RML *p* value	RML versus LML *p* value	Control versus LML *p* value
StO_2 (%)	37.44% ± 11.11	41.56% ± 1.15	10.27% ± 0.27	0.4750	0.0117	0.0130
NIR (%)	66.03% ± 14.67	58.60% ± 12.08	0.27% ± 0.21	0.7000	0.0015	0.0008
TWI (%)	32.58% ± 2.19	37.58% ± 2.97	12.17% ± 3.73	0.1879	0.0001	0.0004
Local lactate (mmol/L)	0.70 ± 0.00	1.33 ± 0.71	3.07 ± 0.84	0.4836	0.0356	0.0091

RML Right medial lob, *LML* left medial lobe, *StO_2* partial oxygen saturation, *NIR%* Near-Infrared Perfusion Index; *TWI%* Tissue Water Index. Data is expressed in mean ± sd. *p* value < 0.05 was considered statistically significant

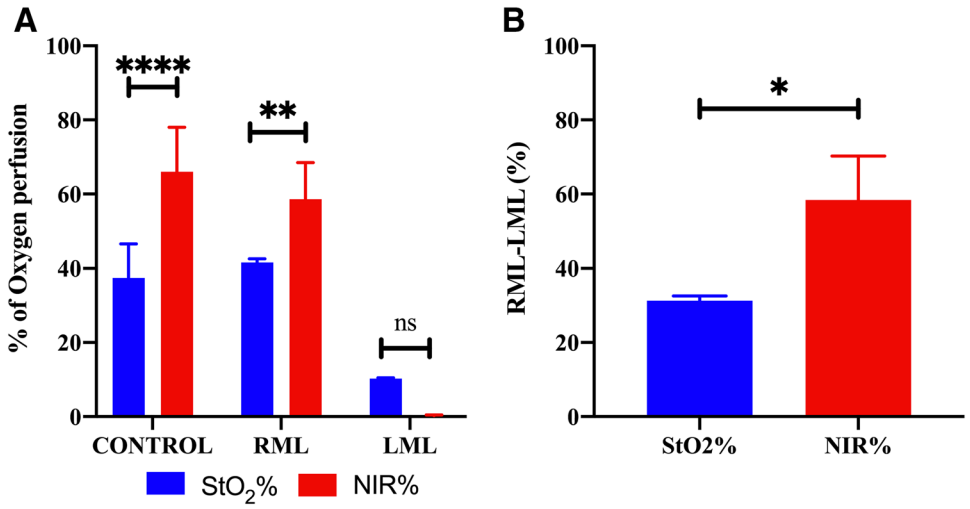

Fig. 3 StO_2% and NIR% comparison. **A** The difference between the two parameters was statistically significantly in the control and in the RML ($p < 0.0001$ and $p = 0.0011$, respectively). **B** The superficial analysis given by StO_2% was less accurate than the NIR% as shown by the difference between the RML and the LML ($p = 0.0326$). Data are expressed as mean ± sd. p value < 0.05 was considered statistically significant

between the RML and the LML (Fig. 3). In addition, the correlation between the local lactate and HSI parameters was statistically significant for (i) local lactate and StO_2% ($r = -0.7805$, 95%CI − 0.95/ − 0.24, $R^2 = 0.6092$, $p = 0.0131$); (ii) local lactate and NIR% ($r = -0.7947$, 95%CI − 0.95/ − 0.27, $R^2 = 0.6316$, $p = 0.0105$); (iii) local lactate and TWI% ($r = -0.7989$, 95%CI − 0.95/ − 0.28, $R^2 = 0.6383$, $p = 0.0098$). Confocal endomicroscopy (Videoclip) performed 1 cm away from the demarcation line in both sides, showed that the perfused region indicated by HSI, i.e., the RML, was characterized by a normal blood circulation, whereas circulation in the LML was absent. Upon injection of fluorescein, the typical emission peak of the fluorophore was noticed as an alteration of the whole HSI spectrum (at around 540 nm). However, this was not interfering with the StO_2% and NIR perfusion indexes that are formed at higher wavelengths (around 800 nm). Finally, a preliminary test for the transection plane was performed. NIR parameter showed low perfusion level in the intraparenchymal plane (Fig. 4).

Discussion

The present acute experiment allowed to demonstrate the feasibility of the HYPER method to intraoperatively identify the demarcation line. The potential clinical relevance of HYPER lies in the accurate discrimination between ischemic and non-ischemic hepatic regions. HSI allowed to clearly identify the demarcation line which could be followed by HSI image superimposition. However, in our setting, the clinically based demarcation line matched with the HYPER-based one in 2 out of 3 cases. The discordant case (Fig. 2B)

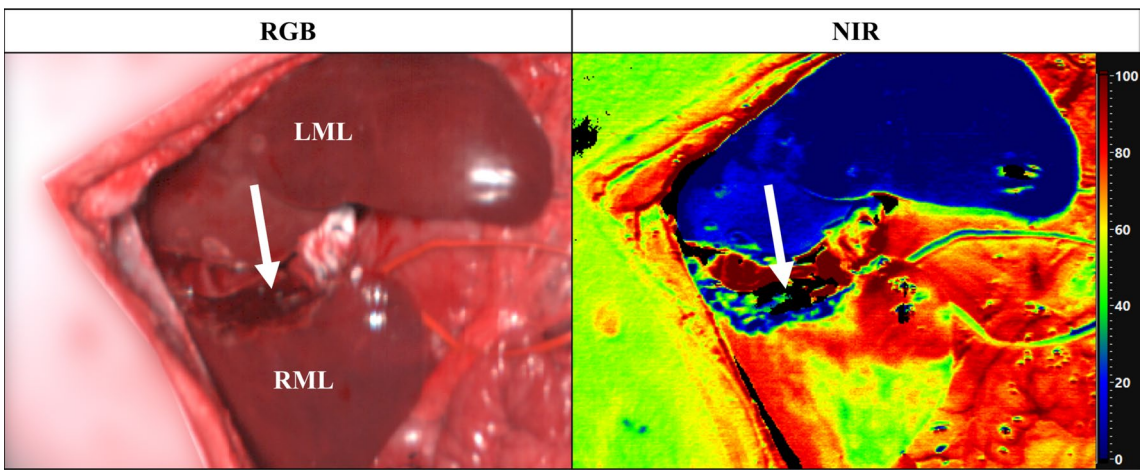

Fig. 4 RGB (left) and NIR perfusion index (right) images of the transection plane. The intraparenchymal HSI analysis of the perfused lobe (RML) shows low level of oxygen perfusion similar to the ischemic lobe (LML) after the resection

provides an example of unclear demarcation, which could be corrected with the HYPER method.

The main advantage of HYPER is the possibility to easily acquire new quantitative images during the procedure, representing the actual perfusion status.

The oxygen perfusion difference between RML and LML calculated by StO_2% on the surface (depth-1mm) was significantly lower when compared to the NIR% which measures in deeper layers (depth 4-6 mm), suggesting that a deeper evaluation of oxygen perfusion could be more accurate. Thus, NIR evaluation through HSI improves the evaluation of the demarcation line compared with the evaluation of the StO_2% and human eye both by being visually sharper and by being quantitatively more discriminating between ischemic and perfused. The high correlation between StO_2%, NIR% and TWI with local lactates confirms the consistency of HSI in discriminating ischemic and non-ischemic areas, with NIR% achieving the highest correlation. In this study, we also performed a preliminary evaluation of the transection plane. This first attempt showed that HSI detected low level of oxygen perfusion in the transection plane of the perfused lobe (RML) (Fig. 4), most likely due to the action of the electrocautery that altered the hyperspectral signal. This aspect will be separately studied in the next experimental steps, in which different HSI set-up and surgical approaches will be tested to avoid the loss of the signal. To the best of our knowledge, HSI has been applied to anatomical left liver resection in a recently published case report [22]. The future transection line, which was marked according to the Cantlie line and the middle hepatic vein, matched the demarcation line, as identified by the same HSI device used in our experimental study. However, the authors did not superimpose the HSI images, which makes difficult to assess the correspondence between the HSI perfusion images and the actual liver surface demarcation line. Additionally, no ground truth tests were performed to assess the accuracy of HSI parameters.

The strong point of our study was the use of superimposition of HSI images onto the RGB video validated by robust metabolic metrics to measure organ perfusion, such as capillary lactates [23–26] and advanced intraoperative microcirculation imaging, such as confocal endomicroscopy [27] which were all concordant with HSI parameters. This supports HYPER as a potential surgical guidance tool despite the multiple limitations of this study, including the low sample size, the acute design, and the focus on the demarcation line rather than on the transection planes. Additionally, the experiments were performed on healthy livers while the real advantages of HSI technology could probably be better defined in clinical conditions (e.g., cirrhosis, steatosis, post-chemotherapy liver injury) that alter the liver surface signal.

Zuzak et al. [16, 28] developed a near-infrared laparoscopic HSI system to help guide laparoscopic surgeons to visualize biliary anatomy. However, there is currently no commercially available HSI-equipped laparoscope. The availability of an integrated laparoscopic HSI system with video rate would obviate for the need of enhanced reality superimposition methods such as HYPER. Clinically, we are planning to evaluate the method in a prospective observational study to establish the accuracy and evaluate the surgical workflow.

Conclusions

In the experimental setting, HSI was accurate in discriminating ischemic from non-ischemic hepatic areas. HYPER could be a suitable intraoperative tool to guide perfusion-based demarcation line assessment and segmentation.

Acknowledgements The authors would like to thank Guy Temporal and Christopher Burel for their assistance in medical English proofreading. The authors are also grateful to Catherine Meunier-Cers for her medical illustration.

Funding This work was funded by the ARC Foundation through the ELIOS (Endoscopic Luminescent Imaging for precision Oncologic Surgery) grant.

Compliance with ethical standards

Disclosures Jacques Marescaux is the President of IRCAD, which is partly funded by KARL STORZ and Medtronic. Michele Diana is member of the scientific board of Diagnostic Green. Michele Diana is the recipient of the ELIOS grant. Takeshi Urade, Eric Felli, Manuel Barberio, Mahdi Al-Taher, Emanuele Felli, Laurent Goffin, Giuseppe Maria Ettorre and Didier Mutter have no conflicts of interest or financial ties to disclose.

References

1. Makuuchi M, Hasegawa H, Yamazaki S (1985) Ultrasonically guided subsegmentectomy. Surg Gynecol Obstet 161:346–350
2. Takasaki K (1998) Glissonean pedicle transection method for hepatic resection: a new concept of liver segmentation. J Hepatobiliary Pancreat Surg 5:286–291
3. Inoue Y, Arita J, Sakamoto T, Ono Y, Takahashi M, Takahashi Y, Kokudo N, Saiura A (2015) Anatomical liver resections guided by 3-dimensional parenchymal staining using fusion indocyanine green fluorescence imaging. Ann Surg 262:105–111
4. Aoki T, Koizumi T, Mansour DA, Fujimori A, Kusano T, Matsuda K, Tashiro Y, Watanabe M, Otsuka K, Murakami M (2020) Ultrasound-guided preoperative positive percutaneous indocyanine green fluorescence staining for laparoscopic anatomical liver resection. J Am Coll Surg 230:e7–e12
5. Ishizawa T, Zuker NB, Kokudo N, Gayet B (2012) Positive and negative staining of hepatic segments by use of fluorescent imaging techniques during laparoscopic hepatectomy. Arch Surg 147:393–394
6. Sakoda M, Ueno S, Iino S, Hiwatashi K, Minami K, Kawasaki Y, Kurahara H, Mataki Y, Maemura K, Uenosono Y, Shinchi H, Natsugoe S (2014) Anatomical laparoscopic hepatectomy for

hepatocellular carcinoma using indocyanine green fluorescence imaging. J Laparoendosc Adv Surg Tech A 24:878–882
7. Mizuno T, Sheth R, Yamamoto M, Kang HS, Yamashita S, Aloia TA, Chun YS, Lee JE, Vauthey JN, Conrad C (2017) Laparoscopic glissonean pedicle transection (Takasaki) for negative fluorescent counterstaining of segment 6. Ann Surg Oncol 24:1046–1047
8. Terasawa M, Ishizawa T, Mise Y, Inoue Y, Ito H, Takahashi Y, Saiura A (2017) Applications of fusion-fluorescence imaging using indocyanine green in laparoscopic hepatectomy. Surg Endosc 31:5111–5118
9. Nomi T, Hokuto D, Yoshikawa T, Matsuo Y, Sho M (2018) A novel navigation for laparoscopic anatomic liver resection using indocyanine green fluorescence. Ann Surg Oncol 25:3982
10. Urade T, Sawa H, Iwatani Y, Abe T, Fujinaka R, Murata K, Mii Y, Man-I M, Oka S, Kuroda D (2020) Laparoscopic anatomical liver resection using indocyanine green fluorescence imaging. Asian J Surg 43:362–368
11. Lu G, Fei B (2014) Medical hyperspectral imaging: a review. J Biomed Opt 19:10901
12. Akbari H, Uto K, Kosugi Y, Kojima K, Tanaka N (2011) Cancer detection using infrared hyperspectral imaging. Cancer Sci 102:852–857
13. Martinez B, Leon R, Fabelo H, Ortega S, Piñeiro JF, Szolna A, Hernandez M, Espino C, O'Shanahan J, Carrera D, Bisshopp S, Sosa C, Marquez M, Camacho R, Plaza ML, Morera J, Callico M (2019) Most relevant spectral bands identification for brain cancer detection using hyperspectral imaging. Sensors (Basel) 19:5481
14. Köhler H, Jansen-Winkeln B, Maktabi M, Barberio M, Takoh J, Holfert N, Moulla Y, Niebisch S, Diana M, Neumuth T, Rabe SM, Chalopin C, Melzer A, Gockel I (2019) Evaluation of hyperspectral imaging (HSI) for the measurement of ischemic conditioning effects of the gastric conduit during esophagectomy. Surg Endosc 33:3775
15. Jansen-Winkeln B, Maktabi M, Takoh JP, Rabe SM, Barberio M, Köhler H, Neumuth T, Melzer A, Chalopin C, Gockel I (2018) Hyperspectral imaging of gastrointestinal anastomoses. Chirurg 89:717–725
16. Zuzak KJ, Naik SC, Alexandrakis G, Hawkins D, Behbehani K, Livingston E (2008) Intraoperative bile duct visualization using near-infrared hyperspectral video imaging. Am J Surg 195:491–497
17. Holmer A, Marotz J, Wahl P, Dau M, Kämmerer PW (2018) Hyperspectral imaging in perfusion and wound diagnostics - methods and algorithms for the determination of tissue parameters. Biomed Tech (Berl) 63:547–556
18. Barberio M, Longo F, Fiorillo C, Seeliger B, Mascagni P, Agnus V, Lindner V, Geny B, Charles AL, Gockel I, Worreth M, Saadi A, Marescaux J, Diana M (2020) HYPerspectral Enhanced Reality (HYPER): a physiology-based surgical guidance tool. Surg Endosc 34:1736–1744
19. Kilkenny C, Browne W, Cuthill IC, Emerson M, Altman DG (2010) Animal research: reporting in vivo experiments: the ARRIVE guidelines. Br J Pharmacol 160:1577
20. Bonaventura JM, Sharpe K, Knight E, Fuller KL, Tanner RK, Gore CJ (2015) Reliability and accuracy of six hand-held blood lactate analysers. J Sports Sci Med 14:203–214
21. Barberio M, Felli E, Seyller E, Longo F, Chand M, Gockel I, Geny B, Swanstrom L, Marescaux J, Agnus V, Diana M (2020) Quantitative fluorescence angiography versus hyperspectral imaging to assess bowel ischemia: a comparative study in enhanced reality. Surgery. https://doi.org/10.1016/j.surg.2020.02.008
22. Sucher R, Athanasios A, Köhler H, Wagner T, Brunotte M, Lederer A, Gockel I, Seehofer D (2019) Hyperspectral Imaging (HSI) in anatomic left liver resection. Int J Surg Case Rep 62:108–111
23. Diana M, Noll E, Diemunsch P, Moussallieh FM, Namer IJ, Charles AL, Lindner V, Agnus V, Geny B, Marescaux J (2015) Metabolism-guided bowel resection: potential role and accuracy of instant capillary lactates to identify the optimal resection site. Surg Innov 22:453–461
24. Diana M, Agnus V, Halvax P, Liu YY, Dallemagne B, Schlagowski AI, Geny B, Diemunsch P, Lindner V, Marescaux J (2015) Intraoperative fluorescence-based enhanced reality laparoscopic real-time imaging to assess bowel perfusion at the anastomotic site in an experimental model. Br J Surg 102:e169–176
25. Diana M, Noll E, Diemunsch P, Dallemagne B, Benahmed MA, Agnus V, Soler L, Barry B, Namer IJ, Demartines N, Charles AL, Geny B, Marescaux J (2014) Enhanced-reality video fluorescence: a real-time assessment of intestinal viability. Ann Surg 259:700–707
26. Diana M, Halvax P, Dallemagne B, Nagao Y, Diemunsch P, Charles AL, Agnus V, Soler L, Demartines N, Lindner V, Geny B, Marescaux J (2014) Real-time navigation by fluorescence-based enhanced reality for precise estimation of future anastomotic site in digestive surgery. Surg Endosc 28:3108–3118
27. Diana M, Noll E, Charles AL, Diemunsch P, Geny B, Liu YY, Marchegiani F, Schiraldi L, Agnus V, Lindner V, Swanstrom L, Dallemagne B, Marescaux J (2017) Precision real-time evaluation of bowel perfusion: accuracy of confocal endomicroscopy assessment of stoma in a controlled hemorrhagic shock model. Surg Endosc 31:680–691
28. Zuzak KJ, Naik SC, Alexandrakis G, Hawkins D, Behbehani K, Livingston EH (2007) Characterization of a near-infrared laparoscopic hyperspectral imaging system for minimally invasive surgery. Anal Chem 79:4709–4715

Terms and Conditions

Springer Nature journal content, brought to you courtesy of Springer Nature Customer Service Center GmbH (“Springer Nature”).
Springer Nature supports a reasonable amount of sharing of research papers by authors, subscribers and authorised users (“Users”), for small-scale personal, non-commercial use provided that all copyright, trade and service marks and other proprietary notices are maintained. By accessing, sharing, receiving or otherwise using the Springer Nature journal content you agree to these terms of use (“Terms”). For these purposes, Springer Nature considers academic use (by researchers and students) to be non-commercial.
These Terms are supplementary and will apply in addition to any applicable website terms and conditions, a relevant site licence or a personal subscription. These Terms will prevail over any conflict or ambiguity with regards to the relevant terms, a site licence or a personal subscription (to the extent of the conflict or ambiguity only). For Creative Commons-licensed articles, the terms of the Creative Commons license used will apply.
We collect and use personal data to provide access to the Springer Nature journal content. We may also use these personal data internally within ResearchGate and Springer Nature and as agreed share it, in an anonymised way, for purposes of tracking, analysis and reporting. We will not otherwise disclose your personal data outside the ResearchGate or the Springer Nature group of companies unless we have your permission as detailed in the Privacy Policy.
While Users may use the Springer Nature journal content for small scale, personal non-commercial use, it is important to note that Users may not:

1. use such content for the purpose of providing other users with access on a regular or large scale basis or as a means to circumvent access control;
2. use such content where to do so would be considered a criminal or statutory offence in any jurisdiction, or gives rise to civil liability, or is otherwise unlawful;
3. falsely or misleadingly imply or suggest endorsement, approval , sponsorship, or association unless explicitly agreed to by Springer Nature in writing;
4. use bots or other automated methods to access the content or redirect messages
5. override any security feature or exclusionary protocol; or
6. share the content in order to create substitute for Springer Nature products or services or a systematic database of Springer Nature journal content.

In line with the restriction against commercial use, Springer Nature does not permit the creation of a product or service that creates revenue, royalties, rent or income from our content or its inclusion as part of a paid for service or for other commercial gain. Springer Nature journal content cannot be used for inter-library loans and librarians may not upload Springer Nature journal content on a large scale into their, or any other, institutional repository.
These terms of use are reviewed regularly and may be amended at any time. Springer Nature is not obligated to publish any information or content on this website and may remove it or features or functionality at our sole discretion, at any time with or without notice. Springer Nature may revoke this licence to you at any time and remove access to any copies of the Springer Nature journal content which have been saved.
To the fullest extent permitted by law, Springer Nature makes no warranties, representations or guarantees to Users, either express or implied with respect to the Springer nature journal content and all parties disclaim and waive any implied warranties or warranties imposed by law, including merchantability or fitness for any particular purpose.
Please note that these rights do not automatically extend to content, data or other material published by Springer Nature that may be licensed from third parties.
If you would like to use or distribute our Springer Nature journal content to a wider audience or on a regular basis or in any other manner not expressly permitted by these Terms, please contact Springer Nature at

onlineservice@springernature.com